

## ORIGINAL ARTICLE

# Astrocyte reactivity in a mouse model of *SCN8A* epileptic encephalopathy

Jeremy A. Thompson<sup>1,2</sup>  | Raquel M. Miralles<sup>1,2</sup> | Eric R. Wengert<sup>1,2</sup>  |  
Pravin K. Wagley<sup>1</sup> | Wenxi Yu<sup>3</sup>  | Ian C. Wenker<sup>1</sup>  | Manoj K. Patel<sup>1,2</sup>

<sup>1</sup>Department of Anesthesiology,  
University of Virginia Health System,  
Charlottesville, VA, USA

<sup>2</sup>Neuroscience Graduate Program,  
University of Virginia, Charlottesville,  
VA, USA

<sup>3</sup>Department of Human Genetics,  
University of Michigan, Ann Arbor, MI,  
USA

## Correspondence

Manoj K. Patel, Department of  
Anesthesiology, University of Virginia  
Health System, Charlottesville, VA, USA.  
Email: [mkp5u@virginia.edu](mailto:mkp5u@virginia.edu).

## Funding information

Citizens United for Research in Epilepsy;  
Foundation for the National Institutes  
of Health, Grant/Award Number: R01  
NS103090, R01 NS120702 and NS034509

## Abstract

**Objective:** *SCN8A* epileptic encephalopathy is caused predominantly by de novo gain-of-function mutations in the voltage-gated sodium channel Na<sub>v</sub>1.6. The disorder is characterized by early onset of seizures and developmental delay. Most patients with *SCN8A* epileptic encephalopathy are refractory to current anti-seizure medications. Previous studies determining the mechanisms of this disease have focused on neuronal dysfunction as Na<sub>v</sub>1.6 is expressed by neurons and plays a critical role in controlling neuronal excitability. However, glial dysfunction has been implicated in epilepsy and alterations in glial physiology could contribute to the pathology of *SCN8A* encephalopathy. In the current study, we examined alterations in astrocyte and microglia physiology in the development of seizures in a mouse model of *SCN8A* epileptic encephalopathy.

**Methods:** Using immunohistochemistry, we assessed microglia and astrocyte reactivity before and after the onset of spontaneous seizures. Expression of glutamine synthetase and Na<sub>v</sub>1.6, and K<sub>ir</sub>4.1 channel currents were assessed in astrocytes in wild-type (WT) mice and mice carrying the N1768D *SCN8A* mutation (D/+).

**Results:** Astrocytes in spontaneously seizing D/+ mice become reactive and increase expression of glial fibrillary acidic protein (GFAP), a marker of astrocyte reactivity. These same astrocytes exhibited reduced barium-sensitive K<sub>ir</sub>4.1 currents compared to age-matched WT mice and decreased expression of glutamine synthetase. These alterations were only observed in spontaneously seizing mice and not before the onset of seizures. In contrast, microglial morphology remained unchanged before and after the onset of seizures.

**Significance:** Astrocytes, but not microglia, become reactive only after the onset of spontaneous seizures in a mouse model of *SCN8A* encephalopathy. Reactive astrocytes have reduced K<sub>ir</sub>4.1-mediated currents, which would impair their ability to buffer potassium. Reduced expression of glutamine synthetase would modulate the availability of neurotransmitters to excitatory and inhibitory neurons. These deficits in potassium and glutamate handling by astrocytes could

This is an open access article under the terms of the [Creative Commons Attribution-NonCommercial-NoDerivs](https://creativecommons.org/licenses/by-nc-nd/4.0/) License, which permits use and distribution in any medium, provided the original work is properly cited, the use is non-commercial and no modifications or adaptations are made.

© 2021 The Authors. *Epilepsia Open* published by Wiley Periodicals LLC on behalf of International League Against Epilepsy.

exacerbate seizures in *SCN8A* epileptic encephalopathy. Targeting astrocytes may provide a new therapeutic approach to seizure suppression.

#### KEYWORDS

astrocytes, epilepsy, glutamine synthetase,  $K_{ir}4.1$ , microglia,  $Na_v1.6$ , sodium channels

## 1 | INTRODUCTION

De novo missense mutations of the gene *SCN8A*, which encodes the voltage-gated sodium channel  $Na_v1.6$  are associated with *SCN8A* epileptic encephalopathy.<sup>1</sup> Clinical features include seizure onset between 4 and 18 months of age, developmental delay after seizure onset, epilepsy with multiple seizure types, and sudden unexpected death in epilepsy (SUDEP) in 10% of cases.<sup>2</sup> The expression of  $Na_v1.6$  is predominantly neuronal, with high expression concentrated at the axon initial segments (AIS) and nodes of Ranvier where it promotes neuronal excitability.<sup>3-5</sup>

Most neurologic disorders, including epilepsy, involve not just neuronal dysfunction but also glial dysfunction. Astrocytes, in particular, play critical roles in maintaining ion and neurotransmitter homeostasis to ensure proper neuronal function.<sup>6</sup> During instances of insult to the brain astrocytes undergo a process termed reactive astrogliosis.<sup>7</sup> Reactive astrocytes display altered morphology, physiology, and gene expression profile compared with astrocytes in the healthy brain, contributing to disease pathology. Several studies have demonstrated that manipulations which produce reactive astrocytes can promote neuronal hyperexcitability<sup>8</sup> or lead to the development of seizures.<sup>9</sup> Astrocyte-specific deletion of either *KCNJ10*, encoding the inward rectifying potassium channel  $K_{ir}4.1$ ,<sup>10</sup> or inhibition of the glutamate degradation enzyme glutamine synthetase (GS), facilitate the development of spontaneous seizures in mouse models.<sup>11</sup> Reactive astrocytes commonly downregulate these critical genes, which could contribute to brain pathology.<sup>6</sup> Moreover, reactive astrocytes are present in human resected tissue from patients suffering from mesial temporal lobe epilepsy (MTLE) and mutations in *KCNJ10* are causative for EAST syndrome (epilepsy, ataxia, sensorineural deafness, and tubulopathy), characterized by epilepsy.<sup>12,13</sup>

Microglia are also thought to be involved in epilepsy. In several models of temporal lobe epilepsy (TLE), microglia become reactive and contribute to seizures by the release of proinflammatory cytokines (IL-1 $\beta$  and TNF) which are proconvulsant and microglial specific knockout of the *TSC1* gene results in microglial reactivity and the development of spontaneous seizures.<sup>14</sup> Microglia may also have roles in regulating the ectopic neurogenesis and synaptic pruning that occurs in epilepsy.<sup>14</sup>

#### Key Points

- Astrocytes, but not microglia, become reactive in spontaneously seizing mice expressing the human *SCN8A* mutation N1768D.
- Astrocyte reactivity is not observed at a time point before the onset of spontaneous seizures even though increases in neuronal excitability have been initiated and audiogenic seizures can be induced.
- Reactive astrocytes have reduced  $K_{ir}4.1$  channel currents suggesting an impairment in  $K^+$  ion uptake.
- Reactive astrocytes have reduced glutamine synthetase expression suggesting impairments in glutamate homeostasis.
- Astrocytes do not express  $Na_v1.6$  indicating that the physiological changes observed in astrocytes are in response to increases in neuronal excitability.

In this study, we investigated whether microglia and astrocyte reactivity were associated with seizures in the N1768D mouse model of *SCN8A* encephalopathy. This model bears the first described patient point mutation, p.Asn1768Asp, and recapitulates key aspects of the disease, including the development of spontaneous seizures and an increased risk of sudden death.<sup>1,5</sup> We show that astrocytes become reactive in the cortex and hippocampus of spontaneously seizing mutant mice and display reduced  $K_{ir}4.1$  currents, indicating an impairment in their ability to regulate extracellular  $K^+$ . Interestingly, prior to the onset of seizures, astrocytes remained quiescent and displayed unaltered  $K_{ir}4.1$  currents. Astrocytes in spontaneously seizing mutant mice also exhibited reduced glutamine synthetase expression, the enzyme necessary for the conversion of glutamate to glutamine, indicating an impairment in glutamate processing. Surprisingly, microglial morphology was unchanged prior to and after the onset of spontaneous seizures. These deficits in the homeostatic functions of astrocytes, but not microglia, could contribute to the development of seizures in *SCN8A* encephalopathy,

implicating a role for astrocytes in the pathology of this disease.

## 2 | MATERIALS AND METHODS

### 2.1 | Animals

All experiments were performed using C57BL/6J WT mice (JAX:000664), transgenic Tg(Aldh111-EGFP,-DTA) D8Rth/J mice (JAX:026033), and *Scn8a*<sup>N1768D</sup> knock-in mice, referred to as D/+.<sup>5,15</sup> All experiments performed on mice were conducted in compliance with the guidelines established by the National Institutes of Health's *Guide for the Care and Use of Laboratory Animals* and were approved by the University of Virginia's Institute of Animal Care and Use Committee. Both male and female mice were used in experiments. D/+ mice were genotyped as previously described.<sup>3</sup> To identify astrocytes Aldh111-EGFP and D/+ mice were crossed to create Aldh111-EGFP:D/+ mice. All mice were maintained on a 12-hour light/dark cycle and allowed access to food and water ad libitum.

### 2.2 | Immunohistochemistry

Brain tissue for immunohistochemistry was processed as follows. Mice were anesthetized and transcardially perfused with 10 mL ice-cold 1× Dulbecco's phosphate-buffered saline (DPBS) followed by 10 mL ice-cold 4% paraformaldehyde (PFA). Sagittal brain sections were immersed in 4% PFA for 2 hours at 4°C then stored in 1× DPBS with 0.1% sodium azide. Brains were embedded in 2% agarose and 40 μm sagittal sections were obtained using a vibratome (Leica VT1200). The following antibodies were used: rabbit polyclonal to GFAP at 1:400 (Abcam, 7260), chicken polyclonal to GFAP at 1:1000 (Abcam, 4674), goat polyclonal to IBA1 at 1:500 (Abcam, 5076), chicken polyclonal to GFP at 1:1000 (Abcam, ab13970), rabbit polyclonal to glutamine synthetase at 1:400 (Abcam, ab176562), and rabbit polyclonal to Na<sub>v</sub>1.6 at 1:100 (Alomone, ASC-009). Primary antibodies were diluted in 2% goat or donkey serum depending on the secondary antibody (Jackson ImmunoResearch) and 0.1% Triton-X (Sigma-Aldrich). Sections (40 μm) were stained free-floating in primary antibody on a shaker at 4°C overnight. Sections were washed twice with 1× DPBS and 0.1% Triton-X. Secondary antibodies were used at 1:1000 and diluted in 2% goat or donkey serum and 0.1% Triton-X. Sections were incubated in secondary antibodies for 1 hour at room temperature on a shaker. All secondary antibodies were obtained from Invitrogen and

used according to the primary antibody being detected. Tissues were counterstained with NucBlue™ Fixed Cell ReadyProbes™ Reagent (DAPI) (Thermo Fisher, catalog #R37606) included in the secondary antibody solution. Tissues were mounted on slides using AquaMount (Polysciences, Inc).

### 2.3 | Quantification of immunohistochemistry

Imaging was performed on a Zeiss LSM 710 confocal microscope with a 20× or 63× objective. We used 3, 4, or 6 slices per mouse (field of view: FOV) to assess the percent area covered of respective immunoreactivity. During image acquisition microscope settings remained constant for WT and D/+ mice. Quantification of percent area covered was performed using ImageJ. The same threshold was applied to images from WT and D/+ mice. For Sholl analysis, brain slices were stained with the microglia/macrophage marker IBA1 and 20× images of cortical regions were acquired with the same settings for WT and D/+ mice. Fifty microglia were analyzed per mouse with 3 mice per group (WT and D/+).

### 2.4 | Brain slice preparation for electrophysiology

Preparation of acute brain slices for electrophysiology experiments was modified from standard protocols previously described.<sup>16</sup> Mice were anesthetized with isoflurane and decapitated. The brains were rapidly removed and kept in chilled ACSF (0°C) containing (in mmol/L): 125 NaCl, 2.5 KCl, 1.25 NaH<sub>2</sub>PO<sub>4</sub>, 2 CaCl<sub>2</sub>, 1 MgCl<sub>2</sub>, 0.5 L-ascorbic acid, 10 glucose, 25 NaHCO<sub>3</sub>, and 2 pyruvate oxygenated with 95% O<sub>2</sub> and 5% CO<sub>2</sub>. Horizontal brain slices (300 μm) of WT and D/+ mice were obtained using a vibratome (Leica VT1200) and were constantly oxygenated with 95% O<sub>2</sub> and 5% CO<sub>2</sub> throughout the preparation. Once sectioning was complete, sulforhodamine-101 (SR101) was added to the aCSF to a final dilution of 1 μmol/L.<sup>17</sup> Slices were incubated in SR101 for 20 minutes at 34°C. Slices were then transferred to aCSF without SR101 for 10 minutes at 34°C to allow removal of excess SR101, before being stored at room temperature in oxygenated aCSF.

### 2.5 | Astrocyte patch clamp recording

During recording, slices were held in a chamber perfused with heated (32°C), oxygenated aCSF. Astrocytes were

identified based on uptake of SR101 using epifluorescent microscopy (Hamamatsu) and morphology using a Zeiss Axioskop 2 FS Plus microscope. Borosilicate glass pipettes (OD 1.0 mm, ID 0.58 mm, WPI) were pulled using a Brown-Flaming puller (Model P97; Sutter Instruments). Pipettes had resistances between 4 and 6 M $\Omega$  when filled with an internal solution of (in mmol/L): 130 KCl, 2 MgCl<sub>2</sub>, 10 HEPES, 5 EGTA, 2 Na<sub>2</sub>ATP, 0.5 CaCl<sub>2</sub> with pH set to 7.3.<sup>18</sup> Measurements were made in whole-cell patch clamp configuration using an Axopatch 700B amplifier (Molecular Devices, pCLAMP 10.6 software) and a Digidata 1322A (Molecular Devices). To analyze potassium (K<sup>+</sup>) currents, whole-cell patched astrocytes were voltage-clamped at -80 mV and stepped from -160 to 100 mV in 20 mV increments, first in aCSF without barium chloride (BaCl<sub>2</sub>), then with the addition of 100  $\mu$ mol/L BaCl<sub>2</sub> to the bath. Barium-sensitive currents were determined by subtraction of current traces in the presence of BaCl<sub>2</sub> from baseline recordings in the absence of BaCl<sub>2</sub>.

## 2.6 | Noninvasive seizure monitoring by video/EEG

To monitor spontaneous seizures, D/+ mice underwent stereotaxic (Kopf, Inc) surgery to implant EEG headsets (Plastics1, Inc). Surgeries were performed in accordance with the Animal Care and Use Committee guidelines at the University of Virginia, and as previously described.<sup>19</sup> Briefly, anesthesia was induced with 5% and maintained with 0.5%-3% isoflurane. A midline skin incision was made over the skull for electrode placement over the left and right parietal cortices. Implantation of electrodes into the brain can result in both astrocytic and microglial activation, so we used EEG leads that were attached to the outer surface of the skull and did not penetrate the brain. These leads and the EEG headset were secured on top of the skull with dental cement. Mice were allowed to recover for a minimum of 2 days and were then housed in custom chambers with food and water *ad libitum*. EEG headsets were connected via custom cables to swivels above the chambers, allowing unrestrained movement. EEG signals were amplified at 2000 $\times$  and bandpass filtered between 0.3 and 100 Hz, with an analogue amplifier (Neurodata Model 12, Grass Instruments Co.). Biosignals were digitized with a Powerlab 16/35 and recorded using LabChart 7 software (AD Instruments, Inc) at 1 kS/s. Video acquisition was performed by multiplexing four miniature night vision-enabled cameras and then digitizing the video feed with a Dazzle Video Capture Device (Corel, Inc) and recorded at 30 frames per second with LabChart 7 software in tandem with biosignals. Seizures were identified by cortical spike wave discharges and commensurate seizure

behaviors that were all considered at least stage 5 on the modified Racine Scale.<sup>20</sup> A subset of mice did not receive surface EEG implantation, but were only video monitored for the presence or absence of seizure behaviors in the same way. Only mice that had on average 2-3 seizures per day for 2-4 consecutive days were used in this study.

## 2.7 | Data analysis

Clampfit software version 10.7 was used to analyze the electrophysiological recordings. Sholl analysis was performed in ImageJ using the Sholl analysis plugin.<sup>21</sup> Data represent means  $\pm$  standard deviation (SD). Statistical significance was determined using Student's *t* test or a standard one-way or two-way ANOVA followed by Sidak multiple comparisons (GraphPad Prism 8).

## 3 | RESULTS

### 3.1 | Astrocytes become reactive in spontaneously seizing SCN8A mutant mice

Increases in the expression of the cytoskeletal protein glial fibrillary acidic protein (GFAP) is indicative of astrocyte reactivity. We therefore assessed the percent area stained for GFAP in adult WT and D/+ mice that were confirmed to be spontaneously seizing. In WT mice, few cortical astrocytes expressed GFAP (Figure 1A,A'; n = 5 mice). In contrast, in spontaneously seizing adult D/+ mice, there was widespread GFAP expression in cortical astrocytes, indicative of reactivity (Figure 1B,B',C; Table 1; n = 5 mice). In addition to the cortex, there was also a significant increase in GFAP expression in hippocampal astrocytes from spontaneously seizing D/+ mice (Figure 1E,E',F; n = 5 mice) compared to WT (Figure 1D,D'; Table 1; n = 5 mice). The increase in GFAP in cortical and hippocampal astrocytes from seizing D/+ mice could be explained by either an increase in individual astrocyte GFAP expression or by an increase in the number of cortical and hippocampal astrocytes. Since GFAP is not uniformly expressed by all astrocytes and is only found in the astrocyte primary processes and labels astrocyte somas poorly, using GFAP to accurately assess astrocyte cell numbers is not ideal. To overcome this, we used mice which express GFP under the ALDH1L1 promoter<sup>22</sup> (Aldh1l1-EGFP:D/+) to selectively label astrocytes in the brain and address whether the increase in GFAP expression was due to an increase in astrocyte numbers. We observed no increase in the number of GFP-labeled astrocytes per FOV (6 per mouse) in either the cortex (Figure 1G-I; n = 5 mice) or hippocampus (Figure 1J-L; n = 5 mice) of spontaneously seizing D/+

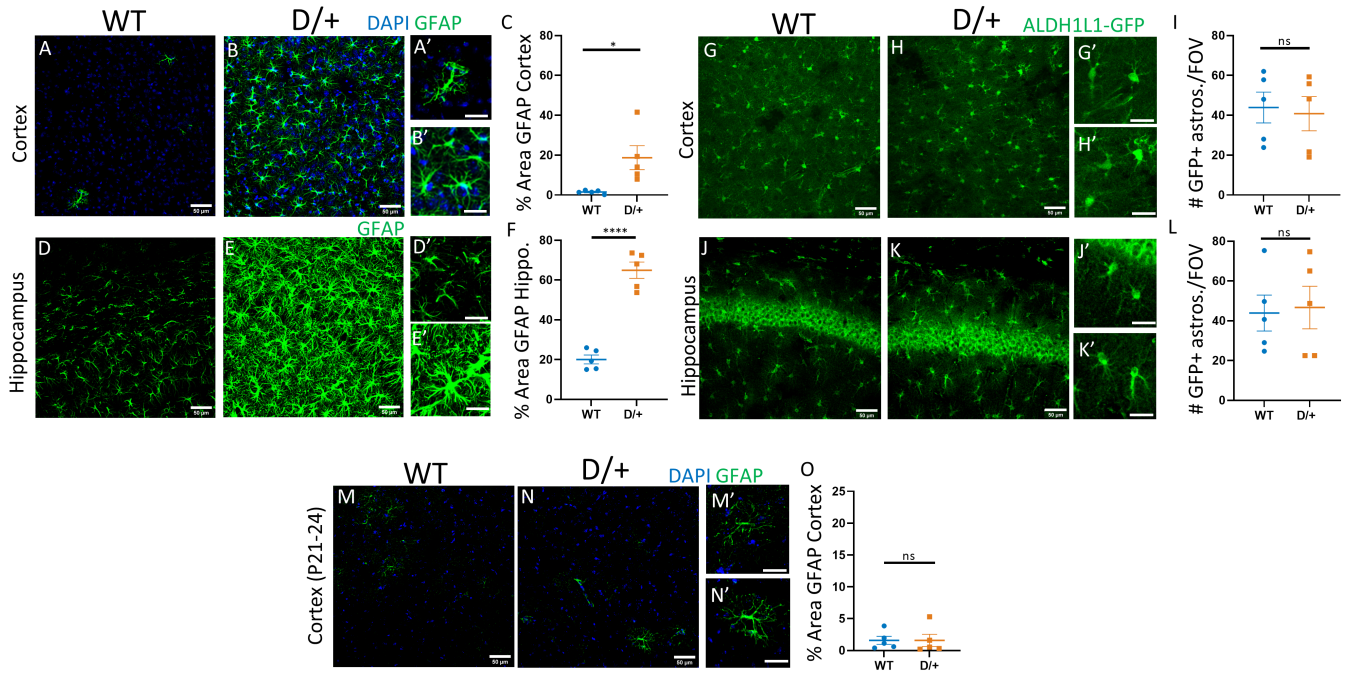


**FIGURE 1** Astrocytes become reactive after the onset of spontaneous seizures. Few cortical astrocytes express GFAP (green) in adult wild-type (WT) mice (A, A'). In contrast, GFAP (green) staining in spontaneously seizing D/+ mouse cortex showed an increase in reactive astrocytes (B, B'). A similar pattern of increased GFAP (green) staining was observed in the hippocampus of spontaneously seizing D/+ mice (E, E') compared with WT (D, D'). Comparison of GFAP expression as percent area covered between WT and D/+ mice in cortex (C) (WT:  $n = 5$  mice and D/+ :  $n = 5$  mice,  $P$ -value = .0215, Student's  $t$  test) and hippocampus (F) (WT:  $n = 5$  mice and D/+ :  $n = 5$  mice,  $P$ -value < .0001, Student's  $t$  test; 3 fields of view (FOV) per mouse). The overall number of astrocytes in the cortex and hippocampus was assessed in ALDH1L1-GFP mice (6 FOV per mouse). Comparison of the number of GFP<sup>+</sup> astrocytes per FOV in 20x confocal images in the cortex (G and H) and hippocampus (J and K) of ALDH1L1-GFP mice is quantified in (I and L) (WT:  $n = 5$  mice and D/+ :  $n = 5$  mice,  $P$ -value = .7935 for cortex (I): WT:  $n = 5$  mice and D/+ :  $n = 5$  mice,  $P$ -value = .8464 for hippocampus (L), Student's  $t$  test). Few cortical astrocytes express GFAP in pre-seizing age (P21-P24) mice irrespective of genotype (M and N). Quantification of GFAP expression in pre-seizing age mice (O) (WT:  $n = 5$  mice and D/+ :  $n = 5$  mice,  $P$ -value = .5476, Student's  $t$  test; 3 FOV per mouse). Scale bar = 50  $\mu$ m, for insets 25  $\mu$ m

**TABLE 1** Summary statistics for GFAP, GFP, and GS quantification

Staining	Brain region	WT	D/+	$P$ value/test
GFAP	Cortex	1.48 $\pm$ 0.39% ( $n = 5$ )	18.71 $\pm$ 6.03% ( $n = 5$ )	$P = .0215$ Students $t$ test
	Hippocampus	20.05 $\pm$ 2.25% ( $n = 5$ )	64.93 $\pm$ 4.08% ( $n = 5$ )	$P < .0001$ Students $t$ test
	Cortex P21-P24	1.60 $\pm$ 0.63% ( $n = 5$ )	1.60 $\pm$ 0.96% ( $n = 5$ )	$P = .5476$ Students $t$ test
GFP	Cortex	43.93 $\pm$ 7.73 ( $n = 5$ )	40.80 $\pm$ 8.57 ( $n = 5$ )	$P = .7935$ Students $t$ test
	Hippocampus	43.87 $\pm$ 9.01 ( $n = 5$ )	46.67 $\pm$ 10.71 ( $n = 5$ )	$P = .8464$ Students $t$ test
Glutamine synthetase	Cortex	75.75 $\pm$ 7.55% ( $n = 7$ )	20.15 $\pm$ 7.33% ( $n = 6$ )	$P = .0002$ Students $t$ test
	Hippocampus	74.45 $\pm$ 5.69% ( $n = 7$ )	27.64 $\pm$ 11.24% ( $n = 6$ )	$P = .0005$ Students $t$ test

mice when compared to WT age-matched controls, suggesting that there was no change in the total number of astrocytes present (Table 1).

Previous studies have shown that D/+ mice are susceptible to audiogenic seizures and have hyper-excitable neurons at time points before the onset of spontaneous seizures which occurs between 8 and 16 weeks postnatal.<sup>3,23</sup> To explore whether astrocyte reactivity occurred before spontaneous seizure onset, we examined the percent area covered by GFAP expression in young WT ( $n = 5$ ) and D/+ ( $n = 5$ ) mice (P21-24; 3 FOV per mouse). In young, nonseizing D/+ mice, there was no difference in cortical (Figure 1M-O) or hippocampal (data not shown) GFAP expression indicating a lack of astrocyte reactivity prior to seizure onset (Table 1).

### 3.2 | Microglial reactivity is not associated with SCN8A epileptic encephalopathy

Microglia are the resident immune cells of the brain, as such, they are uniquely poised to respond to insults or alterations of brain homeostasis by becoming reactive. Reactive microglia are characterized by a change in morphology including reduced arbor complexity and have been detected in mouse models of seizures and in epileptic human resected tissue.<sup>24,25</sup> Reactive microglia exhibit a reduction in process complexity with distance from the soma which can be assessed using Sholl analysis. Staining of microglia with IBA1 showed no change in microglia morphology in preseizing age D/+ mice (Figure 2B) or in spontaneously seizing adult D/+ mice (Figure 2E) compared to age-matched WT mice (Figure 2A,D) ( $n = 3$  WT and 3 D/+ mice, 50 cells per mouse; 3 FOV per mouse,  $P$ -value = .8156 for young mice and  $P$ -value = .7013 for seizing mice, two-way ANOVA, with Sidak multiple

comparisons). No changes in process complexity with distance from soma were detected in either preseizing D/+ mice (Figure 2C) or spontaneously seizing D/+ mice (Figure 2F) compared to age-matched WT controls.

### 3.3 | Astrocytes in spontaneously seizing SCN8A mice display reduced $K_{ir}4.1$ currents

Astrocyte reactivity is associated with the downregulation of genes/proteins involved in the homeostatic functions of astrocytes such as the inward rectifying  $K_{ir}4.1$  channel. The  $K_{ir}4.1$  channel mediates astrocytic uptake of extracellular  $K^+$  that is released following neuronal repolarization after action potentials. Due to the importance of astrocytic  $K_{ir}4.1$  channels to buffer  $K^+$  and its potential to be downregulated in reactive astrocytes, we explored  $K_{ir}4.1$  currents in astrocytes from young preseizing, as well as adult spontaneously seizing D/+ mice. In preseizing mice (P23-P28), there were no significant differences in the total or  $K_{ir}4.1$  currents between WT and D/+ mice (Figure 3A,B,E,F) (WT;  $n = 11$ , 3 mice and D/+;  $n = 9$ , 3 mice;  $P$ -value = .2162 for total current and  $P$ -value = .0722 for  $BaCl_2$ -sensitive current, two-way ANOVA with Sidak multiple comparisons). In contrast, in spontaneously seizing adult D/+ mice, the total current (Figure 3C,D) and  $K_{ir}4.1$  current (Figure 3G,H) amplitudes in reactive astrocytes were significantly reduced by 30% and 36%, respectively (WT;  $n = 10$ , 3 mice and D/+;  $n = 17$ , 3 mice;  $P$ -value = .0085 for total current and  $P$ -value = .0245 for  $BaCl_2$ -sensitive current, two-way ANOVA with Sidak multiple comparisons). These data are suggestive of a disruption in the astrocytic  $K^+$  buffering capacity in seizing D/+ mice. Interestingly, a trend for an increase in the total and  $K_{ir}4.1$  current was observed in young, preseizing D/+ mice.

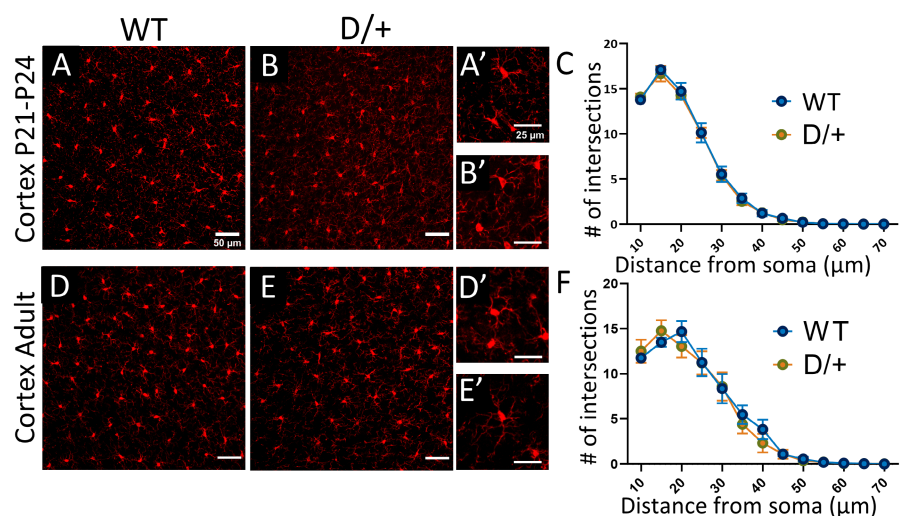


**FIGURE 2** Microglia remain nonreactive in seizing D/+ mice. Cortical microglia, identified by IBA1 expression, in young (A) and adult (D) wild-type (WT) mice compared with young, preseizing (B) and spontaneously seizing adult (E) D/+ mice. Sholl analysis of microglia (IBA1) in WT and D/+ mice (C, F) ( $n = 3$  mice per group; 4 FOV per mouse, 50 cells per mouse, with error bars representing SD,  $P$ -value = .8156 (C) and 0.7013 (F)). Scale bar = 50  $\mu$ m, for insets 25  $\mu$ m

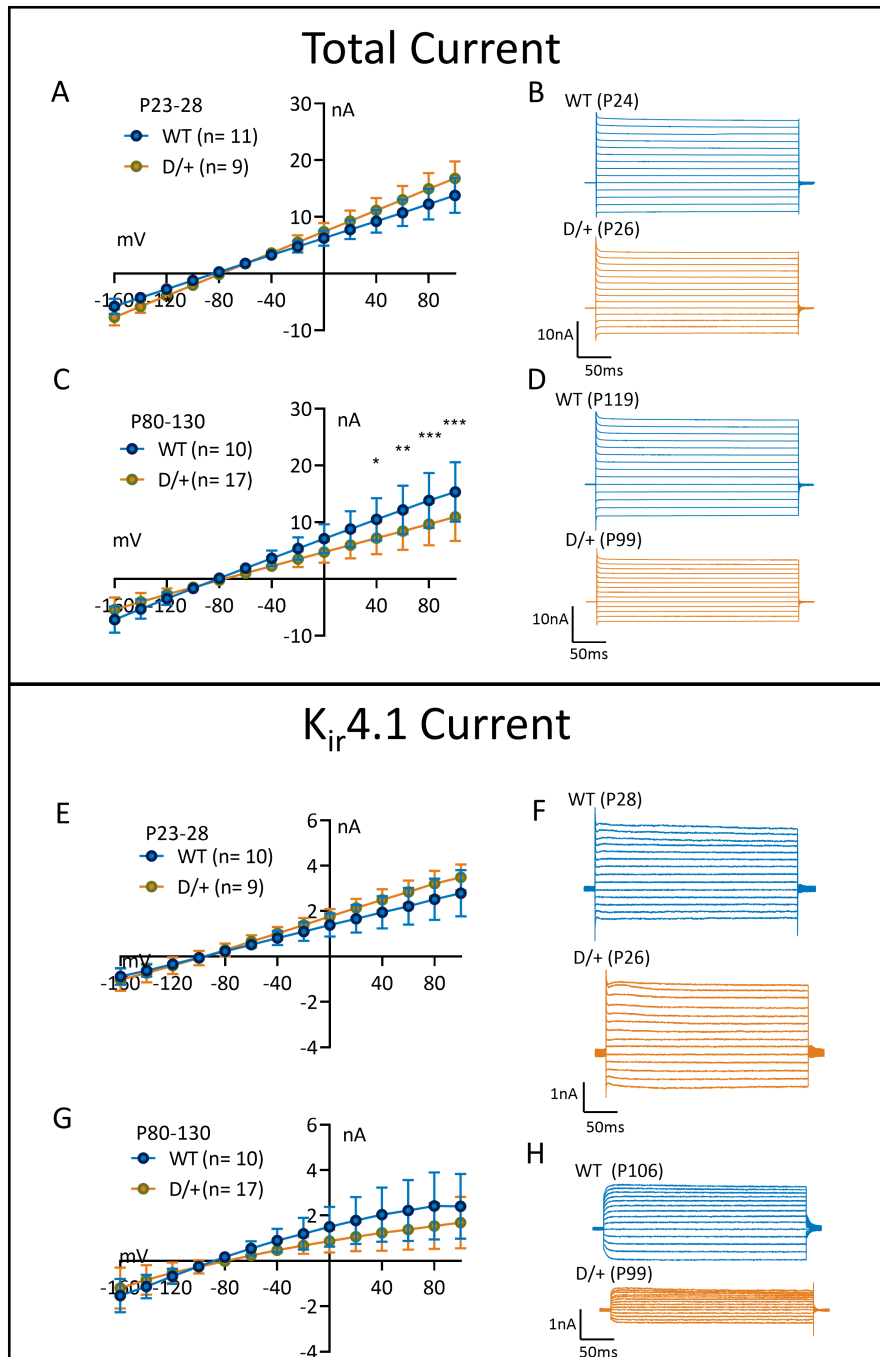


**FIGURE 3** Astrocytes in seizing D/+ mice have reduced  $K_{ir}4.1$  currents. Current/voltage (I/V) plot of total current in young (P23-28) (A) wild-type (WT) and D/+ mice (WT: n = 11, 3 mice and D/+ : n = 9, 3 mice,  $P$ -value = .2162) cortical astrocytes with representative current traces (B). (C) I/V plot of total current in adult (P80-P130) WT and spontaneously seizing D/+ mice (WT: n = 10, 3 mice and D/+ : n = 17, 3 mice,  $P$ -value = 0.0085) with representative traces (D). (E) I/V plot of  $BaCl_2$  sensitive  $K_{ir}4.1$  current in young WT and D/+ mice (WT: n = 10, 3 mice and D/+ : n = 9, 3 mice,  $P$ -value = .0722) with representative traces (F). (G) I/V plot of  $BaCl_2$  sensitive  $K_{ir}4.1$  current in adult WT and spontaneously seizing D/+ mice (WT: n = 10, 3 mice and D/+ : n = 17, 3 mice,  $P$ -value = .0245) with representative current traces (H). Data represent mean  $\pm$  SD. All statistical tests were two-way ANOVA with Sidak multiple comparisons

### 3.4 | Expression of glutamine synthetase is reduced in spontaneously seizing *SCN8A* mice

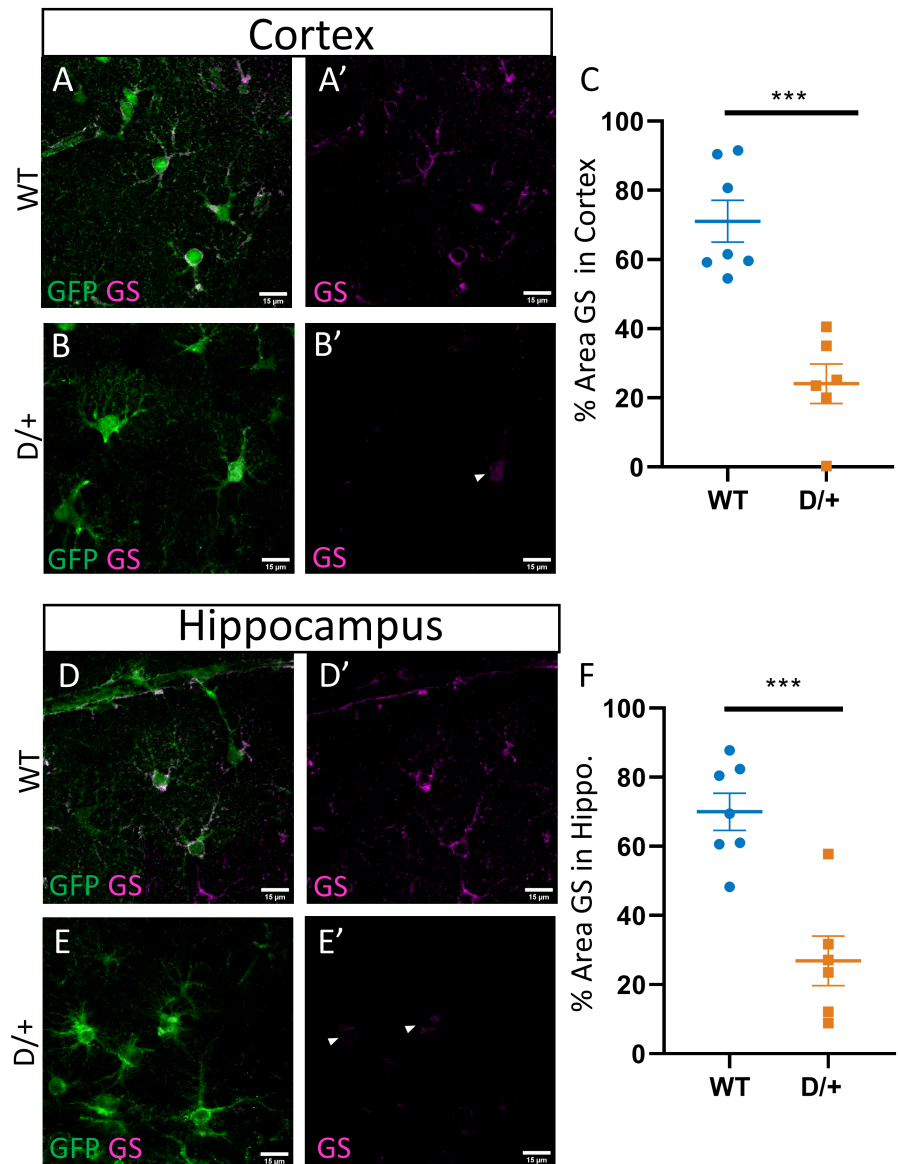
Another important function of astrocytes is the uptake of glutamate and its conversion to glutamine, a precursor for both glutamate and GABA synthesis.<sup>6</sup> This conversion is carried out by the enzyme glutamine synthetase (GS), which is necessary to supply neurons with neurotransmitter precursors and to prevent the reversal of astrocyte glutamate transporters and the release of glutamate from astrocytes. Staining of GS, as defined as percent area covered, was reduced in cortical (Figure 4A-C)

and hippocampal (Figure 4D-F) astrocytes from spontaneously seizing D/+ (n = 6) mice compared to WT (n = 7) mice (Table 1; 4 FOVs per mouse). These results indicate that glutamate handling is likely impaired in spontaneously seizing D/+ mice and could contribute to pathology in this model.

### 3.5 | Astrocytes do not express the voltage-gated sodium channel, $Na_v1.6$

Previous studies have suggested that astrocytes express  $Na_v1.6$ .<sup>26-28</sup> Since *SCN8A* encephalopathy is caused by

**FIGURE 4** Glutamine synthetase (GS) expression is reduced in spontaneously seizing D/+ mice. Immunohistochemistry of glutamine synthetase (GS), magenta, in astrocytes in 40  $\mu\text{m}$  fixed sections of brains from wild-type (WT) cortex and hippocampus (A, D) and spontaneously seizing D/+ mouse cortex and hippocampus (B, E; 4 FOV per cortex and 3 FOV per hippocampus). White arrow heads indicate faint GS labeling in D/+ astrocytes. Green staining represents ALDH1L1-GFP staining of astrocytes. Comparison of the percent of the total area in the FOV covered by GS staining in the cortex (C) and hippocampus (F) of WT and spontaneously seizing D/+ mice ( $n = 7$  WT and  $n = 6$  D/+ mice, Student's *t* test, with error bars representing SD, *P*-value = .0002 for cortex and *P*-value = .0005 for hippocampus. Data represent (mean  $\pm$  SD). Scale bars = 15  $\mu\text{m}$



mutations in *SCN8A*, we investigated whether astrocytes in spontaneously seizing D/+ mice express  $\text{Na}_v1.6$  using immunolabeling techniques. As expected,  $\text{Na}_v1.6$  labeled neuronal somata (asterisks) in WT (Figure 5A:  $n = 3$  mice) and D/+ (Figure 5B:  $n = 3$  mice) mice. However,  $\text{Na}_v1.6$  did not colocalize with the astrocyte reporter GFP fluorescence in the cortex or hippocampus (data not shown). Despite *SCN8A* encephalopathy being caused by mutations in *SCN8A*, our data suggest that astrocytes do not express  $\text{Na}_v1.6$  and their dysfunction in this disease is likely secondary to aberrant neuronal activity caused by neuronal expression of the mutated  $\text{Na}_v1.6$ .

## 4 | DISCUSSION

*SCN8A* encephalopathy is caused primarily by gain-of-function mutations in the neuronal sodium

channel  $\text{Na}_v1.6$  and causes severe, early-onset seizures and SUDEP.<sup>29</sup> Due to the neuronal expression of  $\text{Na}_v1.6$  mechanistic studies into *SCN8A* encephalopathy have focused on the impact of mutations on the excitability of excitatory and inhibitory neurons. However, there is growing appreciation for the involvement of other cell types, principally astrocytes and microglia, in epilepsy pathology.<sup>6,14</sup> In the current study, we sought to investigate alterations in microglia and astrocyte morphology before and after the onset of spontaneous seizures in a knock-in mouse model carrying the human *SCN8A* mutation N1768D. We found that (1) astrocytes, but not microglia, become reactive in spontaneously seizing mice, (2) astrocyte reactivity is not observed at a time point before the onset of spontaneous seizures even though increases in neuronal excitability at this earlier time point have been reported,<sup>3</sup> (3) reactive astrocytes have reduced  $\text{K}_{ir}4.1$  channel currents and reduced GS



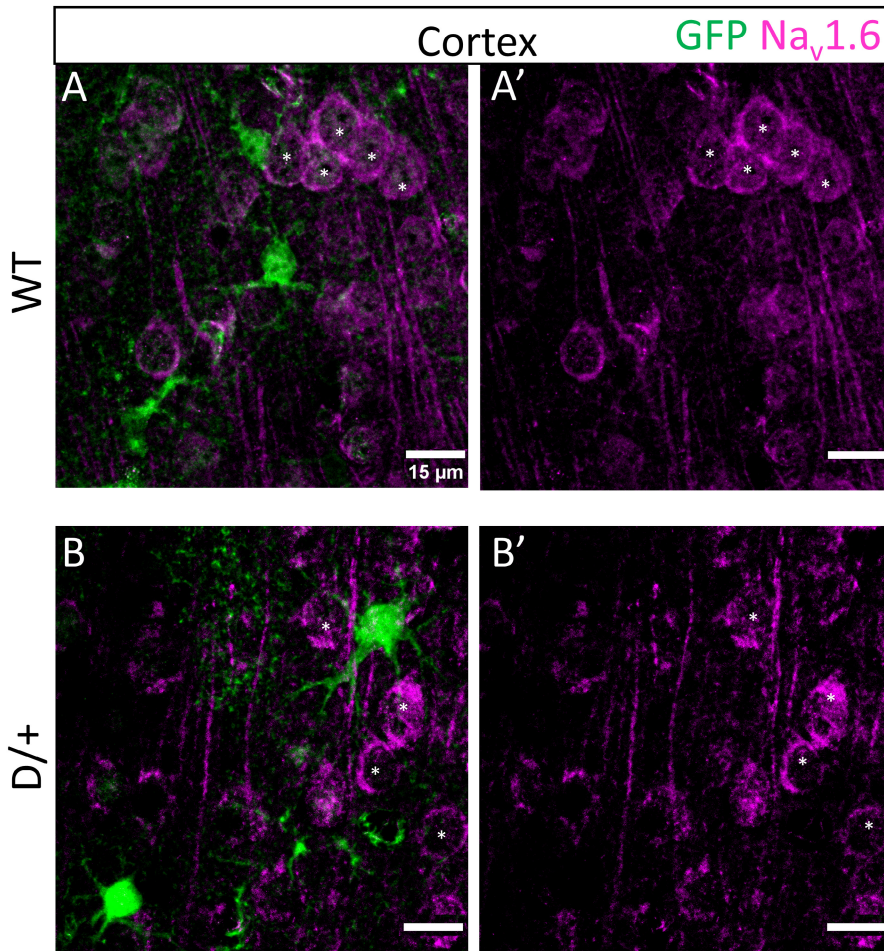


**FIGURE 5** Astrocytes do not express Na<sub>v</sub>1.6 in wild type or in spontaneously seizing D/+ mice. Immunohistochemistry of ALDH1L1-GFP (green) and Na<sub>v</sub>1.6 (magenta) in cortical astrocytes in 40 μm fixed sections of brains from wild-type (A, A': n = 3 mice) and D/+ mice (B, B': n = 3 mice). Na<sub>v</sub>1.6 is expressed in neuronal soma (indicated by asterisk) in neurons, but not colocalized with ALDH1L1-GFP labeled astrocytes. Scale bars = 15 μm

expression suggesting an impairment in K<sup>+</sup> ion uptake and glutamate homeostasis, and (4) astrocytes do not express Na<sub>v</sub>1.6, suggesting that changes in astrocyte physiology are in response to proepileptic alterations in surrounding neuronal networks. This study provides support for a previously unappreciated role for astrocytes in *SCN8A* encephalopathy.

Astrocytes are key cells that function to maintain the homeostasis of the brain through buffering ions, such as K<sup>+</sup>, removing neurotransmitters from the extracellular space, and supporting neurons metabolically, among numerous other roles.<sup>30</sup> Following insults to the brain, astrocytes become reactive and exhibit stereotypic changes in morphology and upregulate cytoskeletal proteins, such as GFAP and vimentin.<sup>7</sup> Despite these stereotypic changes, the term astrocyte “reactivity” refers to a highly heterogeneous process that alters astrocyte physiology in a context-dependent manner.<sup>31</sup> The astrocytic response to CNS insults can be either beneficial or detrimental depending on the type of astrocyte responding (ie, protoplasmic vs. fibrous, cortical vs hippocampal), the type of eliciting event (ie, seizure or infection), and the temporal course of the insult (ie, early- vs late-stage disease).<sup>32,33</sup> The Barres group

demonstrated that astrocytes responding to either systemic LPS injection or middle cerebral artery occlusion (MCAO) become reactive and can be neurotoxic (A1) or neuroprotective (A2), respectively.<sup>31,34</sup> Subsequent work using single-cell RNAseq of isolated astrocytes from various disease models and human samples have revealed astrocyte disease-specific gene expression profiles in Huntington's disease (HD), Alzheimer's disease (AD), and multiple sclerosis that conform neither to the A1 nor the A2 profile.<sup>32,35-37</sup>

While reactive astrocytes can be beneficial as in the case of spinal cord injury by forming a barrier between healthy and necrotic tissue or in *Toxoplasma gondii* infection by producing chemokines to recruit helpful immune cells, reactive astrocytes can also be detrimental.<sup>38,39</sup> A common feature of reactive astrocytes is the downregulation of genes involved in maintaining CNS homeostasis such as K<sub>ir</sub>4.1, aquaporin 4, and neurotransmitter transporters and degrading enzymes.<sup>40</sup> Tong et al (2014) demonstrated that AAV-mediated restoration of reduced K<sub>ir</sub>4.1 expression in reactive striatal astrocytes ameliorated the uncoordinated gait in an HD mouse model. Further, the inability of reactive astrocytes to regulate GABA transmission worsens murine cognition in an AD mouse model.<sup>41</sup>

Loss of the homeostatic functions of astrocytes is the most prominent feature of reactive astrocytes in epilepsy.<sup>6,9,42</sup>

Astrocyte reactivity is often associated with seizures and epilepsy and is considered a “hallmark feature” of MTLE.<sup>6,43</sup> Surgical resection of the glial scar containing reactive astrocytes in epileptic patients alleviates the seizures.<sup>42,44,45</sup> There is debate regarding whether astrogliosis is a cause or consequence of seizures, but growing evidence suggests that astrocyte reactivity alone can lead to seizures<sup>8,9</sup> and mutations in astrocyte-specific genes can lead to epilepsy, as in the case of Alexander’s disease (mutations in *GFAP*) and EAST syndrome (mutations in *KCNJ10*).<sup>46,47</sup> Astrogliosis is often associated with the downregulation of genes necessary for the homeostatic functions of astrocytes such as *KCNJ10*, encoding  $K_{ir}4.1$ , glutamate transporters, and glutamine synthetase.<sup>40,48</sup>

The presence of reactive astrocytes in the D/+ model of *SCN8A* epileptic encephalopathy was previously reported using transcriptome analysis that detected >3-fold elevated expression of the pan-reactive astrocyte transcripts *Gfap*, *Vimentin*, and *Serpina3a* in forebrain of D/+ mice within 24 hours after the onset of seizures, as well as elevated GFAP staining in hippocampus.<sup>34,49</sup> The reactive astrocyte genes *Gfap*, *Vimentin*, and *Serpina3a* were the only astrocyte-specific transcripts detected by Sprissler et al (2017)<sup>31,34,49</sup> from whole-forebrain homogenate and are shared by both A1 and A2 reactive astrocytes. Neurotoxic A1 reactive astrocytes are induced by TNF and IL-1 $\beta$  released from activated microglia.<sup>34</sup> We assessed microglial reactivity in seizing D/+ mice using Sholl analysis and found no evidence for activated microglia. Therefore, the lack of microglial reactivity suggests that reactive astrocytes in seizing D/+ mice are not A1 neurotoxic astrocytes. Conversely, MCAO-induced A2 reactive astrocytes are characterized by cell cycle gene upregulation and the production of neurotrophic factors such as leukemia inhibitory factor (LIF).<sup>31</sup> Our study did not directly address astrocyte proliferation, however, counts of Aldh1L1-eGFP+ cortical and hippocampal astrocytes from WT and seizing D/+ mice demonstrate no change in astrocyte numbers between these two groups. The neurotrophic factor LIF has been implicated in the pilocarpine model of seizures as a proinflammatory cytokine promoting microglia and astrocyte reactivity.<sup>50</sup> LIF knockout mice have reduced microglial and astrocyte reactivity and are more likely to survive pilocarpine-induced seizures than their WT counterparts.<sup>50</sup> In this context, an A2 neurotrophic factor could have a seizure-promoting effect. Our data indicate that reactive astrocytes in seizing D/+ mice do not conform to the A1 or A2 phenotype and future experiments utilizing RNAseq on isolated astrocytes from WT and seizing D/+ mice could clarify the consequences of astrocyte reactivity in *SCN8A* epileptic encephalopathy.

We extend the findings of Sprissler et al (2017) to show that in spontaneously seizing D/+ mice, cortical astrocytes are also reactive and that these reactive astrocytes have reduced  $K_{ir}4.1$  channel currents, with likely deficits in  $K^+$  buffering, and reduced glutamine synthetase expression. We also show that astrocyte reactivity or deficits in  $K_{ir}4.1$  function do not precede the onset of spontaneous seizures even though proexcitatory events have been initiated in medial entorhinal cortex neurons at this time point<sup>3</sup> and mice are susceptible to audiogenic seizures.<sup>23</sup> Metabolic stress has been shown to induce astrogliosis<sup>51</sup> and it is tempting to speculate that astrocytes become reactive as a consequence of increased demand to buffer excess  $K^+$  and glutamate from hyperactive neurons after the onset of spontaneous seizures. Astrocyte reactivity may represent the tipping point in the manifestation of seizures in *SCN8A* encephalopathy, leading to the increase in seizure frequency and eventual death typical of this mouse model.<sup>52</sup>

Astrocyte  $K^+$  buffering through the  $K_{ir}4.1$  channel is essential for proper brain function. Animal models of astrocyte-specific deletion of *KCNJ10* consistently show early mortality with seizures.<sup>10,53-55</sup> Ablation of  $K_{ir}4.1$  impairs  $K^+$  buffering<sup>56</sup> and elevated extracellular  $K^+$  promotes neuronal excitability.<sup>18</sup> In humans, mutations in  $K_{ir}4.1$  cause EAST syndrome.<sup>47</sup> Some of these mutations have been characterized as loss-of-function, thus impairing  $K^+$  buffering through  $K_{ir}4.1$ .<sup>57</sup> In addition to its contribution to  $K^+$  buffering, impairment of  $K_{ir}4.1$  function also reduced glutamate clearance.<sup>10,54</sup> This is likely due to the effect of  $K_{ir}4.1$  on the very negative resting membrane potential of astrocytes and the electrogenic nature of glutamate transporters which rely on the negative membrane potential to import glutamate.<sup>10,30,53,58</sup> Thus, perturbations in  $K_{ir}4.1$  function can contribute to seizures and epilepsy.

Our study also found that glutamine synthetase staining was reduced in spontaneously seizing D/+ mice. Glutamine synthetase is predominantly expressed by astrocytes and its function is critical for the continued uptake of glutamate by glutamate transporters and for the balance of excitatory and inhibitory tone.<sup>6,8,59</sup> In resected tissue from patients suffering from MTLE with hippocampal sclerosis glutamine synthetase expression is greatly reduced<sup>60</sup> and when an inhibitor of glutamine synthetase, methionine sulfoximine, is chronically administered to rats they develop recurrent seizures.<sup>61</sup> Glutamine synthetase expression is also reduced in reactive astrocytes in a slice model of seizure-like activity corresponding to a decrease in inhibitory neurotransmission, a result of a smaller pool of transmitter availability in predominantly GABAergic interneurons.<sup>8</sup>

Lastly, we assessed whether astrocytes in spontaneously seizing D/+ mice express  $Na_v1.6$  since it has been

reported that astrocytes can express Na<sub>v</sub>1.6 in pathological settings.<sup>27,28</sup> However, astrocytes in WT and spontaneously seizing D/+ mice did not express Na<sub>v</sub>1.6. The lack of Na<sub>v</sub>1.6 expression in astrocytes is not surprising and is likely due to the absence of Rbfox RNA-binding protein expression in astrocytes.<sup>62</sup> Rbfox proteins are expressed in neurons and promote the expression of full-length *Scn8a* mRNA transcripts that contain alternative exon 18A. Cells lacking Rbfox proteins, including astrocytes, express alternative exon 18N with an in-frame stop codon that results in nonsense-mediated decay of the *Scn8a* transcript and lack of expression of Na<sub>v</sub>1.6 protein.<sup>62</sup>

In conclusion, the involvement of astrocytes in the pathology of *SCN8A* epileptic encephalopathy is supported by our findings, deepening our understanding of the mechanisms of this type of epilepsy. Our findings suggest that astrocyte functions become impaired in *SCN8A* encephalopathy, contributing to the manifestation of seizures and suggest new therapeutic directions for the treatment of this debilitating disease.

## ACKNOWLEDGMENTS

This work was supported by the National Institutes of Health grants R01 NS103090 and R01 NS120702 (MKP), NS034509 (WY) and Citizens United for Research in Epilepsy (ICW). We acknowledge the important contributions of Prof. Miriam H. Meisler.

## CONFLICT OF INTEREST

None of the authors has any conflict of interest to disclose. Experiments have been performed with all national and international guidelines. The principles outlined in the ARRIVE guidelines, Basel declaration, including the 3R concept, were considered when planning experiments. Our Animal Welfare Assurance Number is A3245-01. We confirm that we have read the Journal's position on issues involved in ethical publication and affirm that this report is consistent with those guidelines.

## ORCID

Jeremy A. Thompson  <https://orcid.org/0000-0001-9937-1888>

Eric R. Wengert  <https://orcid.org/0000-0001-7679-4183>

Wenxi Yu  <https://orcid.org/0000-0003-0911-2706>

Ian C. Wenker  <https://orcid.org/0000-0002-0744-6510>

## REFERENCES

- Veeramah K, O'Brien J, Meisler M, Cheng X, Dib-Hajj S, Waxman S, et al. De novo pathogenic *SCN8A* mutation identified by whole-genome sequencing of a family quartet affected by infantile epileptic encephalopathy and SUDEP. *Am J Hum Genet.* 2012;90(3):502–10.
- Hammer MF, Wagnon JL, Mefford HC, Meisler MH. *SCN8A*-related epilepsy with encephalopathy. In: Adam MP, Ardinger HH, Pagon RA, et al. editors *GeneReviews*® [Internet]. Seattle, WA: University of Washington, Seattle, 2016; p. 1–19. [cited 2021 Feb 10]. Available from <https://www.ncbi.nlm.nih.gov/books/NBK379665/>
- Ottolini M, Barker BS, Gaykema RP, Meisler MH, Patel MK. Aberrant sodium channel currents and hyperexcitability of medial entorhinal cortex neurons in a mouse model of *SCN8A* encephalopathy. *J Neurosci.* 2017;37(32):7643–55.
- Caldwell JH, Schaller KL, Lasher RS, Peles E, Levinson SR. Sodium channel Nav1.6 is localized at nodes of Ranvier, dendrites, and synapses. *Proc Natl Acad Sci USA.* 2000;97(10):5616–20.
- Wagnon JL, Korn MJ, Parent R, Tarpey TA, Jones JM, Hammer MF, et al. Convulsive seizures and SUDEP in a mouse model of *SCN8A* epileptic encephalopathy. *Hum Mol Genet.* 2015;24(2):506–15.
- Patel DC, Tewari BP, Chaunsali L, Sontheimer H. Neuron-glia interactions in the pathophysiology of epilepsy. *Nat Rev Neurosci.* 2019;20(5):282–97.
- Escartin C, Guillemaud O, Carrillo-de Sauvage MA. Questions and (some) answers on reactive astrocytes. *Glia.* 2019;67(12):2221–47.
- Ortinski PI, Dong J, Mungenast A, Yue C, Takano H, Watson DJ, et al. Selective induction of astrocytic gliosis generates deficits in neuronal inhibition. *Nat Neurosci.* 2010;13(5):584–91.
- Robel S, Buckingham SC, Boni JL, Campbell SL, Danbolt NC, Riedemann T, et al. Reactive astrogliosis causes the development of spontaneous seizures. *J Neurosci.* 2015;35(8):3330–45.
- Djukic B, Casper KB, Philpot BD, Chin LS, McCarthy KD. Conditional knock-out of Kir4.1 leads to glial membrane depolarization, inhibition of potassium and glutamate uptake, and enhanced short-term synaptic potentiation. *J Neurosci.* 2007;27(42):11354–65.
- Zhou Y, Dhaher R, Parent M, Hu Q-X, Hassel B, Yee S-P, et al. Selective deletion of glutamine synthetase in the mouse cerebral cortex induces glial dysfunction and vascular impairment that precede epilepsy and neurodegeneration. *Neurochem Int.* 2019;123:22–33.
- Heuser K, Eid T, Lauritzen F, Thoren AE, Vindedal GF, Taubøll E, et al. Loss of perivascular kir4.1 potassium channels in the sclerotic hippocampus of patients with mesial temporal lobe epilepsy. *J Neuropathol Exp Neurol.* 2012;71(9):814–25.
- Mir A, Chaudhary M, Alkhalidi H, Alhazmi R, Albaradie R, Housawi Y. Epilepsy in patients with EAST syndrome caused by mutation in the *KCNJ10*. *Brain Dev.* 2019;41(8):706–15.
- Hiragi T, Ikegaya Y, Koyama R. Microglia after seizures and in epilepsy. *Cells.* 2018;7(4):1–12.
- Jones JM, Meisler MH. Modeling human epilepsy by TALEN targeting of mouse sodium channel *Scn8a*. *Genesis.* 2014;52(2):141–8.
- Wengert ER, Saga AU, Panchal PS, Barker BS, Patel MK. Prax330 reduces persistent and resurgent sodium channel currents and neuronal hyperexcitability of subiculum neurons in a mouse model of *SCN8A* epileptic encephalopathy. *Neuropharmacology.* 2019;158:107699.
- Schnell C, Shahmoradi A, Wichert SP, Mayerl S, Hagos Y, Heuer H, et al. The multispecific thyroid hormone transporter OATP1C1 mediates cell-specific sulforhodamine 101-labeling of hippocampal astrocytes. *Brain Struct Funct.* 2015;220(1):193–203.

18. Tong X, Ao Y, Faas GC, Nwaobi SE, Xu JI, Haustein MD, et al. Astrocyte Kir4.1 ion channel deficits contribute to neuronal dysfunction in Huntington's disease model mice. *Nat Neurosci*. 2014;17(5):694–703.
19. Wagley PK, Williamson J, Skwarzynska D, Kapur J, Burnsed J. Continuous video electroencephalogram during hypoxia-ischemia in neonatal mice. *J Vis Exp*. 2020;2020(160). <https://doi.org/10.3791/61346>
20. Van Erum J, Van Dam D, De Deyn PP. PTZ-induced seizures in mice require a revised Racine scale. *Epilepsy Behav*. 2019;95:51–5.
21. Norris G, Derecki N, Kipnis J. Microglial sholl analysis. *Protoc Exch*. 2014;1–4.
22. Tsai H-H, Li H, Fuentealba LC, Molofsky AV, Taveira-Marques R, Zhuang H, et al. Regional astrocyte allocation regulates CNS synaptogenesis and repair. *Science*. 2012;337(6092):358–62.
23. Wengert ER, Wenker IC, Wagner EL, Wagley PK, Gaykema RP, Shin J-B, et al. Adrenergic mechanisms of audiogenic seizure-induced death in a mouse model of SCN8A encephalopathy. *Front Neurosci*. 2021;15(March):1–16.
24. Wyatt-Johnson SK, Herr SA, Brewster AL. Status epilepticus triggers time-dependent alterations in microglia abundance and morphological phenotypes in the hippocampus. *Front Neurol*. 2017;8(Dec):1–10.
25. Najjar S, Pearlman D, Miller DC, Devinsky O. Refractory epilepsy associated with microglial activation. *Neurologist*. 2011;17(5):249–54.
26. Reese KA, Caldwell JH. Immunocytochemical localization of NaCh6 in cultured spinal cord astrocytes. *Glia*. 1999;26(1):92–6.
27. Zhu H, Zhao Y, Wu H, Jiang N, Wang Z, Lin W, et al. Remarkable alterations of Nav1.6 in reactive astrogliosis during epileptogenesis. *Sci Rep*. 2016;6:38108.
28. Zhu H, Lin W, Zhao Y, Wang Z, Lao W, Kuang P, et al. Transient upregulation of Nav1.6 expression in the genu of corpus callosum following middle cerebral artery occlusion in the rats. *Brain Res Bull*. 2017;132:20–7.
29. Meisler MH, Helman G, Hammer MF, Fureman BE, Gaillard WD, Goldin AL, et al. SCN8A encephalopathy: research progress and prospects. *Epilepsia*. 2016;57(7):1027–35.
30. Verkhratsky A, Nedergaard M. Physiology of astroglia. *Physiol Rev*. 2018;98:239–389.
31. Zamanian JL, Xu L, Foo LC, Nouri N, Zhou L, Giffard RG, et al. Genomic analysis of reactive astrogliosis. *J Neurosci*. 2012;32(18):6391–410.
32. Escartin C, Galea E, Lakatos A, O'Callaghan JP, Petzold GC, Serrano-Pozo A, et al. Reactive astrocyte nomenclature, definitions, and future directions. *Nat Neurosci*. 2021;24:312–25.
33. Matias I, Morgado J, Gomes FCA. Astrocyte heterogeneity: impact to brain aging and disease. *Front Aging Neurosci*. 2019;11:1–18.
34. Liddel SA, Guttenplan KA, Clarke LE, Bennett FC, Bohlen CJ, Schirmer L, et al. Neurotoxic reactive astrocytes are induced by activated microglia. *Nature*. 2017;541(7638):481–7.
35. Al-Dalahmah O, Sosunov AA, Shaik A, Ofori K, Liu Y, Vonsattel JP, et al. Single-nucleus RNA-seq identifies Huntington disease astrocyte states. *Acta Neuropathol Commun*. 2020;8(1):1–21.
36. Grubman A, Chew G, Ouyang JF, Sun G, Choo XY, McLean C, et al. A single-cell atlas of entorhinal cortex from individuals with Alzheimer's disease reveals cell-type-specific gene expression regulation. *Nat Neurosci*. 2019;22(12):2087–97.
37. Wheeler MA, Clark IC, Tjon EC, Li Z, Zandee SEJ, Couturier CP, et al. MAFG-driven astrocytes promote CNS inflammation. *Nature*. 2020;578:593–99.
38. Wanner IB, Anderson MA, Song B, Levine J, Fernandez A, Gray-Thompson Z, et al. Glial scar borders are formed by newly proliferated, elongated astrocytes that interact to corral inflammatory and fibrotic cells via STAT3-dependent mechanisms after spinal cord injury. *J Neurosci*. 2013;33(31):12870–86.
39. Still KM, Batista SJ, O'Brien CA, Oyesola OO, Früh SP, Webb LM, et al. Astrocytes promote a protective immune response to brain *Toxoplasma gondii* infection via IL-33-ST2 signaling. *PLoS Pathog*. 2020;16(10):1–28.
40. Nwaobi SE, Cuddapah VA, Patterson KC, Randolph AC, Olsen ML. The role of glial-specific Kir4.1 in normal and pathological states of the CNS. *Acta Neuropathol*. 2016;132(1):1–21.
41. Dossi E, Vasile F, Rouach N. Human astrocytes in the diseased brain. *Brain Res Bull*. 2018;136:139–56.
42. Xu S, Sun Q, Fan J, Jiang Y, Yang W, Cui Y, et al. Role of astrocytes in post-traumatic epilepsy. *Front Neurol*. 2019;10:1–10.
43. Kim JH. Pathology of epilepsy. *Exp Mol Pathol*. 2001;70(3):345–67.
44. Robel S. Astroglial scarring and seizures: a cell biological perspective on epilepsy. *Neuroscientist*. 2017;23(2):152–68.
45. Hubbard J, Binder DK. *Astrocytes and Epilepsy*. 1st ed. Cambridge, MA: Academic Press Inc.; 2016.
46. Messing A, Brenner M, Feany MB, Nedergaard M, Goldman JE. Alexander disease. *J Neurosci*. 2012;32(15):5017–23.
47. Abdelhadi O, Iancu D, Stanescu H, Kleta R, Bockenbauer D. EAST syndrome: clinical, pathophysiological, and genetic aspects of mutations in KCNJ10. *Rare Dis*. 2016;4(1):1–10.
48. Sheldon AL, Robinson MB. The role of glutamate transporters in neurodegenerative diseases and potential opportunities for intervention. *Neurochem. Int*. 2007;51(6–7):333–55.
49. Sprissler RS, Wagnon JL, Bunton-Stasyshyn RK, Meisler MH, Hammer MF. Altered gene expression profile in a mouse model of SCN8A encephalopathy. *Exp Neurol*. 2017;288:134–41.
50. Holmberg KH, Patterson PH. Leukemia inhibitory factor is a key regulator of astrocytic, microglial and neuronal responses in a low-dose pilocarpine injury model. *Brain Res*. 2006;1075(1):26–35.
51. Sofroniew MV. Astrogliosis perspectives. *Cold Spring Harb Perspect Biol*. 2015;7(2):1–16.
52. Wenker IC, Teran FA, Wengert ER, Wagley PK, Panchal PS, Blizzard EA, et al. Postictal death is associated with tonic phase apnea in a mouse model of sudden unexpected death in epilepsy. *Ann Neurol*. 2021;89(5):1023–35.
53. Neusch C, Papadopoulos N, Müller M, Maletzki I, Winter SM, Hirrlinger J, et al. Lack of the Kir4.1 channel subunit abolishes K<sup>+</sup> buffering properties of astrocytes in the ventral respiratory group: Impact on extracellular K<sup>+</sup> regulation. *J Neurophysiol*. 2006;95(3):1843–52.
54. Kucheryavykh YV, Kucheryavykh LY, Nichols CG, Maldonado HM, Baksi K, Reichenbach A, et al. Downregulation of Kir4.1 inward rectifying potassium channel subunits by RNAi impairs potassium transfer and glutamate uptake by cultured cortical astrocytes. *Glia*. 2007;55(3):274–81.
55. Stewart TH, Eastman CL, Groblewski PA, Fender JS, Verley DR, Cook DG, et al. Chronic dysfunction of astrocytic inwardly rectifying K<sup>+</sup> channels specific to the neocortical epileptic focus after fluid percussion injury in the rat. *J Neurophysiol*. 2010;104(6):3345–60.

56. Haj-Yasein NN, Jensen V, Vindedal GF, Gundersen GA, Klungland A, Ottersen OP, et al. Evidence that compromised K<sup>+</sup> + spatial buffering contributes to the epileptogenic effect of mutations in the human kir4.1 gene (KCNJ10). *Glia*. 2011;59(11):1635–42.
57. Reichold M, Zdebik AA, Lieberer E, Rapedius M, Schmidt K, Bandulik S, et al. KCNJ10 gene mutations causing EAST syndrome (epilepsy, ataxia, sensorineural deafness, and tubulopathy) disrupt channel function. *Proc Natl Acad Sci USA*. 2010;107(32):14490–5.
58. Olsen ML, Sontheimer H. Functional implications for Kir4.1 channels in glial biology: From K<sup>+</sup> + buffering to cell differentiation. *J Neurochem*. 2008;107:589–601.
59. Norenberg MD, Martinez-Hernandez A. Fine structural localization of glutamine synthetase in astrocytes of rat brain. *Brain Res*. 1979;161(2):303–10.
60. Eid T, Thomas MJ, Spencer DD, Rundén-Pran E, Lai J, Malthankar GV, et al. Loss of glutamine synthetase in the human epileptogenic hippocampus: possible mechanism for raised extracellular glutamate in mesial temporal lobe epilepsy. *Lancet*. 2004;363(9402):28–37.
61. Eid T, Ghosh A, Wang Y, Beckstrom H, Zaveri HP, Lee T-S W, et al. Recurrent seizures and brain pathology after inhibition of glutamine synthetase in the hippocampus in rats. *Brain*. 2008;131(8):2061–70.
62. O'Brien JE, Drews VL, Jones JM, Dugas JC, Barres BA, Meisler MH. Rbfox proteins regulate alternative splicing of neuronal sodium channel SCN8A. *Mol Cell Neurosci*. 2012;49(2):120–6. <https://doi.org/10.1016/j.mcn.2011.10.005>

**How to cite this article:** Thompson JA, Miralles RM, Wengert ER, et al. Astrocyte reactivity in a mouse model of SCN8A epileptic encephalopathy. *Epilepsia Open*. 2022;7:280–292. <https://doi.org/10.1002/epi4.12564>